RSC Advances

PAPER

View Article Online
View Journal | View Issue

Cite this: *RSC Adv.*, 2025, **15**, 2078

Isomerization of pirazolopyrimidines to pyrazolopyridines by ring-opening/closing reaction in aqueous NaOH†

Carlos Cifuentes, Nestor Bravo, Daniel Restrepo, Mario Macías and Jaime Portilla *

Received 2nd September 2024
Accepted 24th December 2024

DOI: 10.1039/d4ra06345g

rsc.li/rsc-advances

An isomerization reaction of 7-aryl-3-formylpyrazolo[1,5-*a*]pyrimidines to 5-aroyl-NH-pyrazolo[3,4-*b*]pyridines proceeding with high yields in aqueous NaOH under microwave conditions is reported. This unprecedented transformation occurs by adding and eliminating a water molecule *via* an ANRORC mechanism (adding the nucleophile, ring-opening, and ring-closing) studied using DFT calculations. The product's utility was proved as they have aroyl and NH groups that simple methods and readily available reagents easily modified; likewise, their optical properties were studied, highlighting their high potential as highly emissive modular dyes (φ_F up to 99%). NMR, HRMS, and X-ray diffraction analysis resolved the products' structures.

Introduction

Exploring efficient methods to yield aza-heterocyclic compounds (N–HCs) is essential in organic and medicinal chemistry; this focus is inspired by the high potential to incorporate diverse functionalities into these compounds to expand their scope and pertinency.[1–3] Along these lines, heteroaromatic rings with three or more nitrogen atoms in 5 : 6 fused rings have shown particular interest as they are structural analogs of purines found in various biological and photophysically relevant compounds (Fig. 1a).[4–7] Especially pyrazolo[3,4-*b*]pyridines (PPys), such as the anxiolytic drug tracazolate (**I**), the 5-benzoyl derivative (**II**, inhibitor of CDK2 protein), and the antihypertensive agent riociguat (**III**) are N–HCs that have been explored for their therapeutic potential.[8–11] Likewise, some PPys have been highlighted for their fluorescent properties (typical property of 5 : 6 fused ring[12,13]) in chemosensors discovery (*e.g.*, probe **IV**),[14–16] (Fig. 1b).

The pyrazolo[3,4-*b*]pyridine (PPy) ring formation is achieved through cyclization reactions of 1,3-biselectrophilic pyridines (*e.g.*, 3-acyl-2-halopyridines, route A) with hydrazine derivatives and, to a greater extent, from *N*-substituted aminopyrazoles with 1,3-biselectrophilic reagents (*e.g.*, β-alkoxyenones, route B).[6,15–19] However, by using NH-5-aminopyrazoles in route B, the reaction mainly yields pyrazolo[1,5-*a*]pyrimidines,[5,20] and route A is limited by the poor availability of substrates[6,21] (Fig. 1c). As a result, access to *N*-unsubstituted PPys is limited since most existing examples are route A-based,[6,20,21] and rarer are PPys substituted with an aroyl group at position 5.[8,22–24] Most reports on obtaining 5-aroyl-NH-pyrazolo[3,4-*b*]pyridines are found in pharmaceutical patents,[25] and due to this, finding one article with one derivative was only possible.[20] In that work, the authors react 3-formylchromones **V** with 5-amino-3-methylpyrazole (**VI**) to access the 5-aroyl group by a reaction

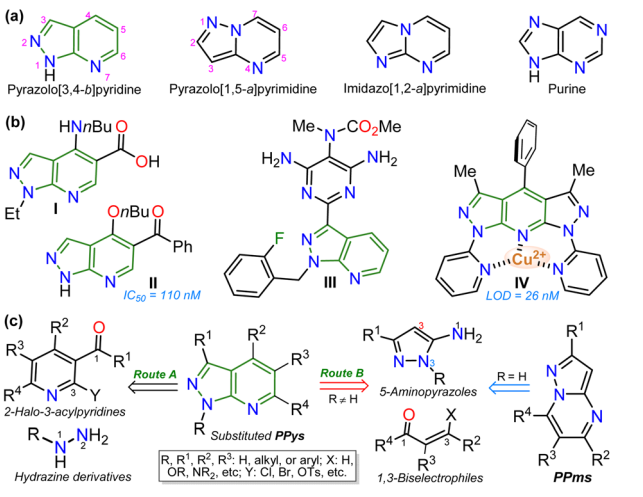

Fig. 1 (a) Structure of aza-heteroaromatic 5 : 6 fused rings with heteroaromatic character. (b) Examples of biological and physically relevant pyrazolo[3,4-*b*]pyridines. (c) Synthesis general of pyrazolo[3,4-*b*]pyridines.

Department of Chemistry, Universidad de Los Andes, Carrera 1 No. 18A-10, Bogotá 111711, Colombia. E-mail: jportill@uniandes.edu.co

† Electronic supplementary information (ESI) available: Experimental details, characterization data, NMR and HRMS charts, crystallographic and theoretical details, and photophysical studies. CCDC: **2a** 2358586, **2b** 2358587, **2b′** 2358589, and **3a** 2358588. For ESI and crystallographic data in CIF or other electronic format see DOI: https://doi.org/10.1039/d4ra06345g

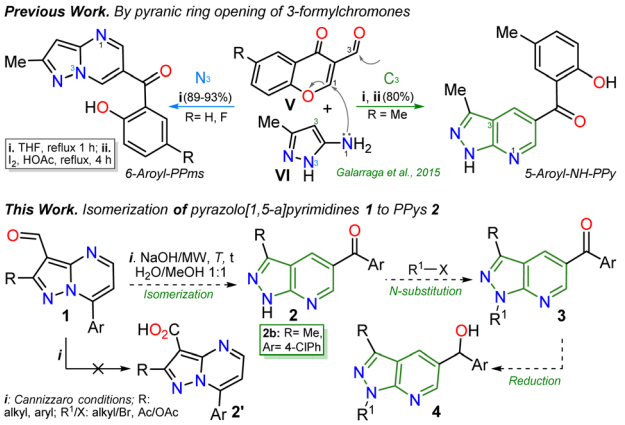

Scheme 1 Synthesis of 5-aroyl-NH-pyrazolopyridines studied in previous work (at the top) and in this work (at the bottom).

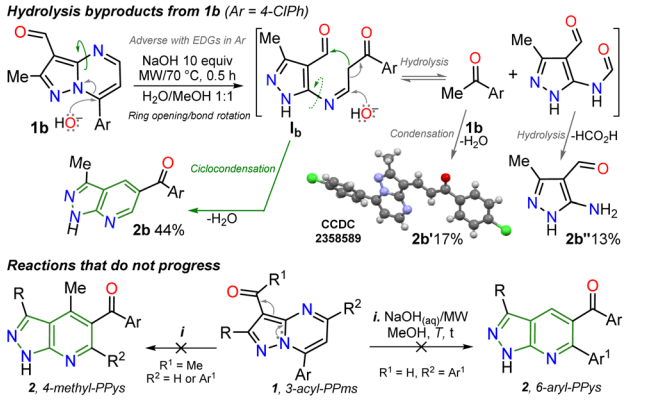

Scheme 2 Highlighted results for the studied isomerization reaction of **1b**.

proceeding with the opening of the pyranic ring in **V**; however, this method has limitations such as the poor availability of substrate, the recurrence of a phenolic moiety in products, and the competence with pyrazolo[1,5-*a*]pyrimidines (Scheme 1a).[20] Importantly, 5-benzoyl-NH-pyrazolo[3,4-*b*]pyridines (similar to **II** in Fig. 1) were obtained in poor global yields (up to ~5%) using synthetic strategies implying more than seven steps with a deprotection protocol for the NH-pyrazolic group.[11]

Inspired by the synthetic applications of pyrazolo[1,5-*a*] pyrimidines under the microwave conditions (MWC) and our investigations in this area,[5,26–28] the Cannizzaro reaction[26–28] on the 3-formyl derivative **1b** was utilized to access the respective carboxylic acid 2′. This acid type could be used in further studies as an N,O-donor ligand in recognition or coordination chemistry, an unusual line in these fused pyrazoles.[5] However, an unexpected but fascinating result was found in the used reaction conditions (excess NaOH) as the isomerization product **2b** was obtained instead of the desired carboxylic acid 2′. Therefore, we aimed to thoroughly study this isomerization reaction to get a novel family of pyrazolo[3,4-*b*]pyridines employing an optimized synthetic approach; we also proposed to examine the practical applicability of this protocol using functionalization strategies and the appropriate photophysical study of some representative derivatives (Scheme 2b). These investigations were proposed as isomerization products would be functionalized with easily modifiable aroyl and NH groups, and 5 : 6 fused rings have evidenced relevant fluorescent properties.[12–16]

Results and discussion

Synthesis

It is important to note that this is the first report on this isomerization reaction class, and due to the strange nature of the transformation, it wasn't easy to establish the structure of **2b**; we achieved it by X-ray diffraction (XRD) analysis (Scheme 2, see ESI† for more details). From these exciting findings, we wonder whether the isomerization could be optimized using the 3-formylpyraolo[1,5-*a*]pyrimidine **1b** (R/Ar = Me/4-ClPh, Scheme 1b) as a model substrate and a high excess NaOH (10 equiv.) at 70 °C for 30 minutes as initial conditions.

The reaction does not progress when developed in water as **1b** is insoluble; thus, the reaction was carried out in water/methanol to improve the substrate solubility under microwave irradiation, obtaining **2b** in 44% yield (Table 1, entry 1 *versus* 2). However, the excess NaOH used also favours the formation of enone **2b′** and the pyrazole derivative **2b″**. This result could be evidence of the ring-opening intermediate **Ib** that also delivered **2b**, also suffers total hydrolysis – *e.g.*, **Ab** is converted to 4-chloroacetophenone that reacts with a second molecule of **1b** – (Scheme 2a). It should be noted that the reaction (*i.e.*, NaOH with substrate **2b**) only works well in H_2O/MeOH due to its better solubility behavior; indeed, the reaction worsens in H_2O/EtOH and does not advance in H_2O/MeCN.

Table 1 Optimization for the isomerization reaction of **1b** to **2b**[a]

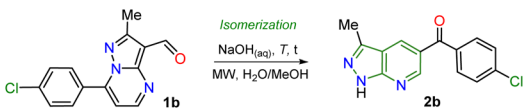

Entry	NaOH (equiv.)	H_2O/MeOH	*t* (min)	*T* (°C)	**2b**, yield (%)
1	10	1 : 0	30	70	NR
2	10	1 : 1	30	70	44
3	10	1 : 1	30	100	68
4	10	1 : 1	30	120	75
5	5	1 : 1	30	100	85
6	5	1 : 1	10	100	87
7	2	1 : 1	5	100	90
8	1	1 : 1	5	100	52
9	1.5	1 : 1	5	100	63
10	2	5 : 1	5	100	Traces
11	2	3 : 1	5	100	44
12	*2*	*2 : 1*	*5*	*100*	*91*
13[b]	2	2 : 1	150	Reflux	61

[a] Reaction conditions: 52 mg of **1b** (0.19 mmol) and NaOH (7.6–76 mg) in 0.7 mL of solvent under microwave conditions; reactions run in a 10 mL sealed tube. [b] Reaction under conventional heating at reflux with a heating mantle in 2 mL of solvent.

We continued the isomerization reaction study by increasing the reaction temperature, and good yields were obtained despite the slight presence of **2b′** and **2b″**. Thus, the amount of base and the reaction time were decreased (entries 3–4 *versus* 5–9), finding excellent results with 2 equivalents of NaOH at 100 °C for 5 minutes as **2b** was obtained in 90% yield (Table 1, entry 7). To achieve a greener protocol, we tried to reduce the MeOH amount, noticing that **1b** was wholly dissolved in a mixture with up to a 2 : 1 ratio of H_2O/MeOH (entries 10–12). Finally, obtaining the pyrazolo[1,5-*a*]pyrimidine **2b** under conventional heating at reflux was also possible but in moderate yield (Table 1, entry 13).

With the optimal conditions established (Table 1, entry 12), we next explored the scope of the isomerization reaction using substrates **1a–l**. Remarkably, excellent tolerance for substituent at positions 2 (Me, *t*Bu, and aryl) and 7 (aryl and hetaryl), with different stereoelectronic natures, was observed. However, substrates bearing electron-donating groups (EDGs) at position C7 (*i.e.*, **1d**, **1g**, **1i**, and **1l**) increase the electron density at this carbon atom[5] (please see ^{13}C NMR data of **1a–l** (ref. 26–28) and LUMO orbital of **1a** in ESI†) to an adverse initial nucleophilic attack decreasing reaction yields (Scheme 2a). For example, the conversion from **1l** to **2l** was only possible under reflux conditions for 48 hours, obtaining the lowest yield (50%) as the substrate's triphenylamine group is highly electron-donating. Curiously, although there was complete conversion, the reaction also offered moderate yields (62–65%) with highly electron-withdrawing groups (EWGs) at position C7 of substrate (as the pyridine ring in **1e** and **1f**); this result is due to the extraction process since **2e** and **2f** are slightly more soluble in aqueous medium than the other PPys (Scheme 3). Unfortunately, highly insoluble substrates (*i.e.*, 7-Ar = 4-O_2NPh, 4-NCPh, or 4-tolyl) or containing another aryl group at position 5 (*i.e.*, 5-Ar = Ph or 4-ClPh) or an acetyl group instead of formyl are resistant to any change under the optimized reaction conditions; this result is probably as they are very polar or more stable molecules by a better π-conjugation[5,28] (Scheme 2b).

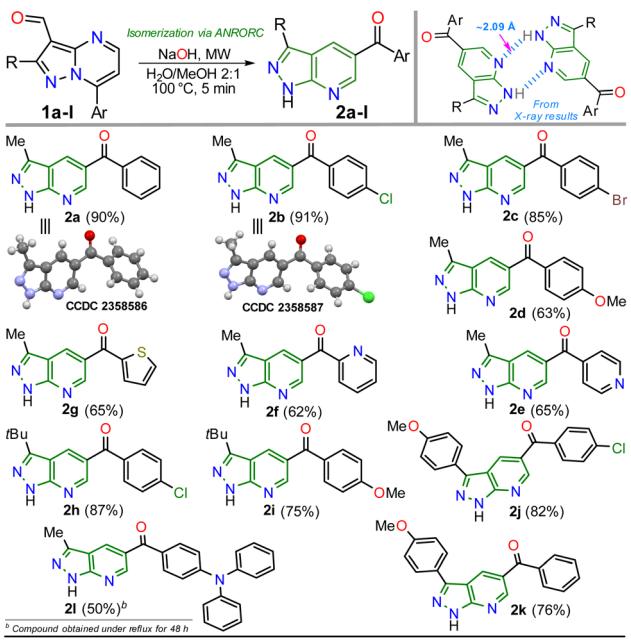

Scheme 3 Scope of the isomerization reaction using substrates **1a–l**.

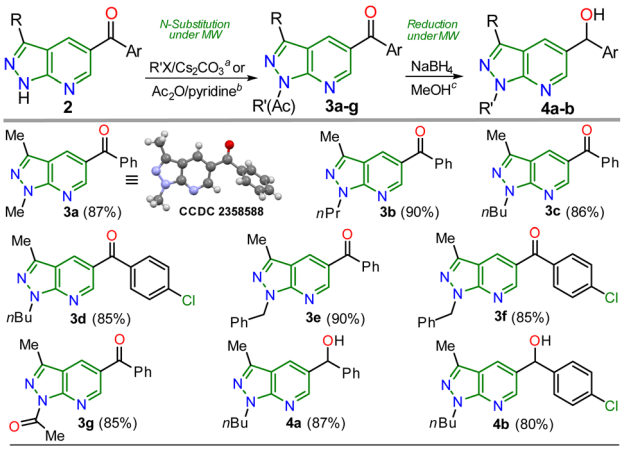

Scheme 4 Synthesis of *N*-substituted 5-aroylpyrazolo[3,4-*b*]pyridines **3a–g** and reduction products (alcohols) **4a–b**.

Once the 5-aroyl-NH-pyrazolo[3,4-*b*]pyridines **2a–l** were obtained, we developed functionalization reactions to access new derivatives with this relevant heterocyclic core, obtaining strategic compounds with a high potential in medicinal and organic chemistry.[20–24] In this way, the *N*-alkylation reaction on the pyrazole moiety was conducted using alkyl halides (2 equiv.) and caesium carbonate (2 equiv.) in MeCN (2 mL) at 80 °C for 15 minutes under MWC, obtaining **3a–f** in high yields (85–90%); the amide ion was previously generated at 50 °C for 3 minutes also under microwave conditions (Scheme 4).

As expected, the acetylation reaction of **2a** (0.25 mmol) with acetic anhydride (2 equiv.) in pyridine (2 mL) at 120 °C for 30 minutes in MWC efficiently afforded the *N*-acetyl derivate **3g** in 85% yield. Ultimately, the reduction reaction of the carbonyl group in **3c–d** was successfully developed using $NaBH_4$ (2 equiv.) in methanol at 100 °C for 5 minutes under MWC, forming alcohols **4a–b** in high yields (80–87%, Scheme 4). Pleasantly, all the obtained pyrazolo[3,4-*b*]pyridines are structurally novel and functional, so they are potentially helpful for new synthetic procedures, allowing their application in various fields of chemistry; for example, compounds **2a–l** could be used as *N*,*N*-donor ligands to access coordination complexes, as observed in the hydrogen bonding interactions found by XRD studies (Scheme 3 and Fig. S48†). Likewise, structures of enone **2b′** (Scheme 2), **2a–b** (Scheme 3), and *N*-methyl derivative **3a** (Scheme 4) were solved using single-crystal XRD analysis.[29] All the obtained compounds (**2b′**, **2b″**, **2a–l**, **3a–g**, and **4a–b**) were characterized through NMR and high-resolution mass spectra (HRMS) analysis (see ESI† for details).

Photophysical studies

During synthetic experiments, we noticed that some products exhibit luminescent properties in solution and solid state under exposure to UV light, mainly the two derivatives with 4-anisyl

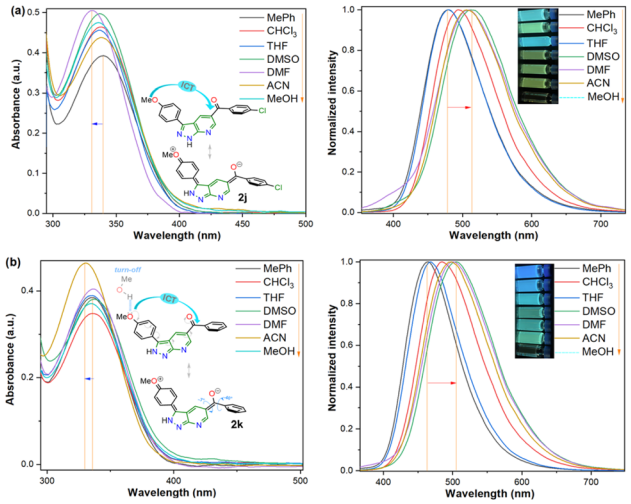

Fig. 2 Absorption (left) and emission (right, $\lambda_{ex} = 335$ nm) spectra and photographs of probes (a) **2j** and (b) **2k** in different solvents (50 μM) at 20 °C.

group (4-MeOPh) at position 3; thus, the photophysical study of **2j–k** was conducted to establish the scope of their donor–π–acceptor molecular architecture (D–π–A or MeO–π–C=O) in organic fluorophores development. Due to their synthetic potential, these results would allow us to document PPys **2j–k** as strategic intermediates of new functional fluorophores, considering some fluorescent dyes bearing pyrazolo[1,5-*a*]pyridine ring.[15,16,30] In addition to the initially observed luminescence, probes **2j–k** were photophysically studied since the 4-anisyl group, bonded to diverse chromophores, has proven helpful in this area, mainly by intramolecular charge transfer (ICT) phenomena using 5 : 6 fused aza-heterocyclic rings.[31–34] In this manner, the absorption and emission spectra of fluorophores **2j–k** were recorded in solvents of different polarity (solvent, Δ*f*): toluene (MePh, 0.013), chloroform ($CHCl_3$, 0.149), tetrahydrofuran (THF, 0.210), dimethylsulfoxide (DMSO, 0.265), *N*,*N*-dimethylformamide (DMF, 0.275), acetonitrile (ACN, 0.306), and methanol (MeOH, 0.309) (Fig. 2 and Table 2).

Compounds **2j–k** displayed absorption spectra with the typical band of $S_0 \rightarrow$ ICT transitions (*i.e.*, MeO → C=O) at around 335 nm with extinction coefficient (ε) values of 7840–10 100 M^{-1} cm^{-1} for **2j** (4-ClBz) and 6940–9280 M^{-1} cm^{-1} for **2k** (Bz). These results revealed a slight blue-shifted and best absorptivity by increasing solvent polarity, with **2j** as the best chromophore due to its higher number of electrons (Fig. 2, left). Both probes exhibited high fluorescence quantum yield (ϕ_F) and brightness ($B = \varepsilon \times \phi_F$) values, mainly in less polar solvents (*e.g.*, $\phi_F = 99\%$ and $B = 7762$ for **2j** in MePh), with a sharp decrease in the emission intensity of **2j** in DMF or ACN (Fig. 2, right). This is owing to the stability of non-emitting excited states, meaning that the energy received by solute is dissipated in non-radiative ways rather than released as light. Polar solvents can help with nonradiative relaxing by creating an environment where vibrational energy can be more efficiently transmitted to the solvent; this reduces the quantity of energy emitted as light, decreasing the fluorescence quantum yield.[35–40] Moreover, both probes displayed significant Stokes shifts (8578–10 582 cm^{-1} for **2j** and 8299–10 856 cm^{-1} for **2k**) with a marked red-shifted by increasing solvent polarity (Fig. 2 and S49,† Table 2).

Importantly, the photophysical properties **2j–k** were dramatically affected in methanol due to strong hydrogen bonding interactions of their anisyl group with solvent molecules ($\phi_F \leq 1\%$). This solvent acts as a fluorescence quencher in **2j–k**, blocking the ICT process to afford energy transfer without light emission; however, this property could be relevant in determining water or ethanol in some organic solvents or distilled spirits (Fig. 2).[36,37] In addition, the Lippert–Mataga plots for **2j–k** illustrate their typical behaviour in the excited states with the variation of orientation polarizability (Δ*f*) of the

Table 2 Photophysical data of 3-(4-anisyl)pyrazolo[3,4-*b*]pyridines **2j–k**[a]

Probe	Solvent[b]	λ_{abs} (nm)	ε (M^{-1} cm^{-1})	λ_{em} (nm)	SS (cm^{-1})	ϕ_F	B ($\varepsilon \times \phi_F$)
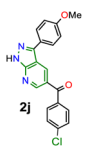 **2j**	MePh	339	7840	478	8578	0.99	7762
	$CHCl_3$	337	9260	493	9389	0.78	7223
	THF	336	9100	479	8885	0.78	7098
	DMSO	338	8740	512	10 054	0.53	4632
	DMF	337	9940	508	9988	0.31	3082
	ACN	331	10 100	507	10 487	0.30	3030
	MeOH	335	9500	519	10 582	0.0069	66
 **2k**	MePh	335	7700	464	8299	0.93	7161
	$CHCl_3$	335	6940	484	9189	0.88	6107
	THF	334	7760	468	8572	0.84	6519
	DMSO	337	7560	503	9792	0.96	7258
	DMF	336	8080	499	9721	0.77	6222
	ACN	330	9280	498	10 222	0.74	6867
	MeOH	334	7400	524	10 856	0.01	74

[a] Quantum yield (ϕ_F) values were determined using Prodan as a standard. Absorbance (ab), fluorescence emission (em), molar absorption coefficient (ε), Stokes shift (SS), and calculated bright (B) data are also shown. [b] Variation of orientation polarizability (Δ*f*): 0.013, 0.149, 0.210, 0.265, 0.275, 0.306, and 0.309, respectively.

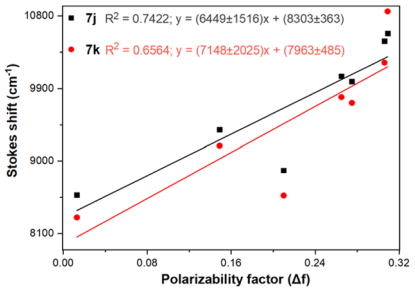

Fig. 3 Lippert–Mataga plots ($\Delta\nu$ *vs.* Δf) for probes **7j–k** in different solvents.

solvent; as expected, they evidenced different interactions with the evaluated solvents, leading to two unique straight-line correlations with positive slopes (Fig. 3). This can be explained as a general solvation effect in low polarity solvents; in contrast, specific interactions like dipole–dipole in polar solvents stabilise the system; it would not be dependable to compute the change in the dipole moment using these numbers due to the low R^2 value, suggesting no strong association polarity factor/Stokes shift. However, from the positive slopes in the graphs, it is possible to see the defined trends according to the slope direction for each probe, demonstrating positive solvatofluorochromism.[35–40]

Accordingly, it is proved that the ICT phenomenon in fluorescent probes **2j–k** favours a good charge separation within these molecules through resonance from the anisyl group towards the carbonyl group (*i.e.*, MeO → C=O). It should be noted that the benzene ring in the aroyl group at position 5 of the aza-heterocyclic core does not greatly affect the ICT process as this ring is not coplanar with the D–π–A system of fluorophores **2j–k** (Fig. 2); this structural characteristic could be determined through the dihedral angles found from crystallographic X-ray diffraction analyses for similar structures (*i.e.*, **2a** and **2b**, Fig. S48 in ESI†). Finally, from the significant photophysical properties found for probes **2j–k** and the good synthetic results involving compounds **2a–l**, **3a–g**, and **4a–b**, we can establish that the heterocyclic core of pyrazolo[3,4-*b*]pyridine is a promisor functional fluorophore; specifically for developing applications in coordination chemistry, diagnostic bioimaging in living systems, chemosensors discovery, photosensitizers, or organic materials science.[13,31–40]

DFT calculations

The primary reaction was studied using density functional theory (DFT) B3LYP/6-311+(d,p) calculations to understand better the mechanism of the discovered reaction with the associated relative free energies (ΔG) by substrate **1a**.[41,42] The relative free energy calculated for the overall reaction is −11.79 kcal mol^{-1}, indicating greater product **2a** stability than substrate **1a** due to the high aromatic character of the pyridine ring in **2a**.[5,6] It is important to note that a negative charge is induced within structures during the reaction due to the medium nature and the initial attack of the hydroxyl anion; however, the isomerization involves the addition and

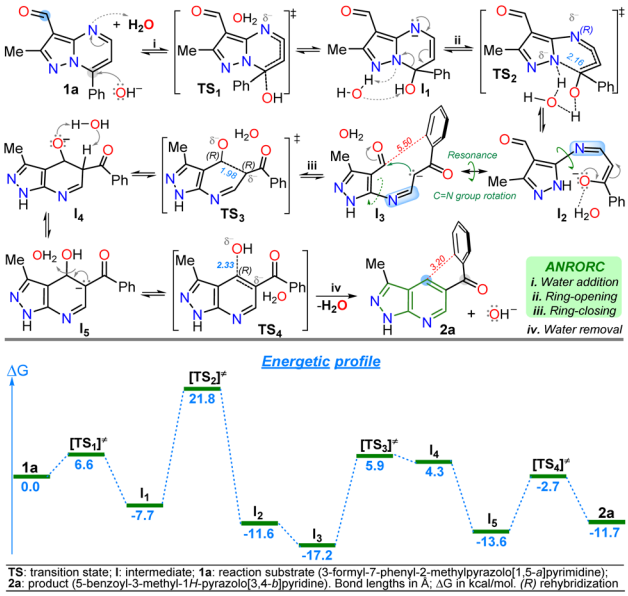

Scheme 5 Proposed mechanism (at the top) for the isomerization reaction of **1a** to **2a** with its respective energetic profile (at the bottom).

elimination of a water molecule through an ANRORC (adding the nucleophile, ring-opening, and ring-closing) mechanism. Implicit water was initially modelled, and explicit modelling of a single water molecule proved crucial in stabilizing transitional states by clustering negative charges within acceptor hydrogen groups along structures. Incorporating a hydroxyl group at position 7 on substrate **1a** exhibits lower energy than the initial structure, implying greater stabilization for intermediate $\mathbf{I_1}$, allowing the pyrimidine ring-opening to find metastable state cause of possible intermediates $\mathbf{I_2}$ and $\mathbf{I_3}$. This study supports that rotation in the imine group of $\mathbf{I_2}$ is favourable, leading to the pyridine ring-closing to afford $\mathbf{I_4}$ by reacting the stabilized carbanion with the C-carbonyl in $\mathbf{I_3}$ (Scheme 5).

The explored mechanism reveals four crucial transition states involving the bonding of the hydroxyl group $\mathbf{TS_1}$, its detachment $\mathbf{TS_4}$, and the isomerization process *via* ring-opening $\mathbf{TS_2}$ and ring-zar[13] closing $\mathbf{TS_3}$. The free energies in $\mathbf{TS_2}$/$\mathbf{TS_3}$ are higher than in $\mathbf{TS_1}$/$\mathbf{TS_4}$, indicating that the most critical reaction steps involve opening the pyrimidine ring and closing the pyridine ring under MWC. The energy levels of structures $\mathbf{TS_3}$ and $\mathbf{I_4}$ are closely matched. Deprotonation of the acidic hydrogen at position 5 of the dihydro-pyridine ring in $\mathbf{I_4}$ reduces the relative free energy, resulting in the discovery of a metastable state $\mathbf{I_5}$ that finally facilitates the formation of a hydroxyl group (base regeneration) to yield the heteroaromatic product **2a** (Scheme 5). Notably, the anionic intermediate $\mathbf{I_3}$ has the lowest energy in the energetic profile, even lower than **2a**, due to the implicit water solvation model used in the presence of the hydroxyl anion; indeed, **2a** has an electronic repulsion between the two rings of the molecule at 3.20 Å in different planes. In contrast, $\mathbf{I_3}$ has larger distances (5.50 Å) between the ring of the aroyl group and the nearest carbon atom that would be part of the fused ring, reducing intramolecular electronic repulsions (Scheme 5 and Fig. S51†).

Conclusions

In summary, a NaOH-mediated isomerization reaction of 7-aryl-3-formylpyrazolo[1,5-*a*]pyrimidines to 5-aroylpyrazolo[3,4-*b*] pyridines was successfully developed under microwave conditions at 100 °C. Eleven isomerization products were obtained in high yields (up to 91%) employing mild reaction conditions in an aqueous medium and cheap reagents. Notably, a mechanistic route for this transformation was also proposed based on DFT calculations and the experimental results; this implies an ANRORC route that started with the hydroxy anion addition at the C7 of the aza-heterocyclic core of the substrate. Additionally, the obtained ketoamines have strategic functional groups (aroyl and NH-heteroaryl) that were easily modified by simple approaches and readily available reagents. The structure of all the obtained compounds was established based on NMR, HRMS, and X-ray diffraction studies. Likewise, the two more luminescent obtained ketoamines were photophysically studied, indicating the utility of the 4-anisyl group and 5 : 6 fused rings in the optoelectronic properties of fluorophores acting through ICT phenomena. Fluorescence quantum yields of up to 99% were obtained with dyes having positive (redshift) solvatofluorochromism, highlighting the high potential of these two compounds as functional fluorophores; for example, as methanol acted as a solvent fluorescence quenching blocking the ICT process in the two tested ketoamines, new applications in sensing water or ethanol in different mediums could be possible.

Data availability

The experimental data, NMR and HRSM spectra, crystallographic and photophysical details (CCDC: **2a** 2358586, **2b** 2358587, **2b′** 2358589, and **3a** 2358588), and computational details have been included in the ESI.

Author contributions

The individuals listed as authors have contributed to developing this manuscript, and no other person was involved. The authors' contributions included: C. C. and N. B. carried out experiments and literature review; D. R. and M. M. carried out computational and XRD studies, respectively; and J. P. the composition of the original draft, supervision, and sources. All authors have read and agreed to the published version of this manuscript.

Conflicts of interest

The authors declare no competing financial interest.

Acknowledgements

The authors gratefully acknowledge the Chemistry Department and Vicerrectoría de Investigaciones at the Universidad de Los Andes for financial support (project INV-2023-162-2810). N.B. acknowledges to Ministerio de Ciencia Tecnología e Innovación (MINCIENCIAS) for a PhD fellowship (Con. 1 to FCTel of SGR). We also recognize S. Ortiz and the High-Performance Computing (HPC) services of Universidad de Los Andes to acquire the mass spectra and access the computational facilities.

Notes and references

1 N. R. Candeias, L. C. Branco, P. M. P. Gois, C. A. M. Afonso and A. F. Trindade, More sustainable approaches for the synthesis of n-based heterocycles, *Chem. Rev.*, 2009, **109**, 2703–2802.
2 S. Kuwata and F. E. Hahn, Complexes Bearing Protic N-Heterocyclic Carbene Ligands, *Chem. Rev.*, 2018, **118**, 9642–9677.
3 Y. Wang, W.-X. Zhang and Z. Xi, Carbodiimide-based synthesis of N-heterocycles: moving from two classical reactive sites to chemical bond breaking/forming reaction, *Chem. Soc. Rev.*, 2020, **49**, 5810–5849.
4 R. Z. U. Kobak and B. Akkurt, Formation and Uses of Imidazo [1,2-a]pyrimidines and Related Compounds: A Review Comprising Years 2000-2021, *J. Turk. Chem. Soc., Sect. A*, 2022, **9**, 1335–1386.
5 J. Portilla, in *Adv. Heterocycl. Chem.*, Elsevier Inc., 2024, 1st edn, pp. 71–138.
6 A. Donaire-Arias, A. M. Montagut, R. P. de la Bellacasa, R. Estrada-Tejedor, J. Teixidó and J. I. Borrell, 1H-Pyrazolo [3,4-*b*]pyridines: Biomedical Applications Synthesis and Biomedical Applications, *Molecules*, 2022, **27**, 2237.
7 S. M. Hoy, Pimitespib: First Approval, *Drugs*, 2022, **82**, 1413–1418.
8 S. B. Bharate, T. R. Mahajan, Y. R. Gole, M. Nambiar, T. T. Matan, A. Kulkarni-Almeida, S. Balachandran, H. Junjappa, A. Balakrishnan and R. A. Vishwakarma, Synthesis and evaluation of pyrazolo[3,4-*b*]pyridines and its structural analogues as TNF-α and IL-6 inhibitors, *Bioorg. Med. Chem.*, 2008, **16**, 7167–7176.
9 J. Mittendorf, S. Weigand, C. Alonso-Alija, E. Bischoff, A. Feurer, M. Gerisch, A. Kern, A. Knorr, D. Lang, K. Muenter, M. Radtke, H. Schirok, K. H. Schlemmer, E. Stahl, A. Straub, F. Wunder and J. P. Stasch, Discovery of riociguat (BAY 63-2521): A potent, oral stimulator of soluble guanylate cyclase for the treatment of pulmonary hypertension, *ChemMedChem*, 2009, **4**, 853–865.
10 M. C. Ríos and J. Portilla, Recent Advances in Synthesis and Properties of Pyrazoles, *Chemistry*, 2022, **4**, 940–968.
11 R. N. Misra, D. B. Rawlins, H. Y. Xiao, W. Shan, I. Bursuker, K. A. Kellar, J. G. Mulheron, J. S. Sack, J. S. Tokarski, S. D. Kimball and K. R. Webster, 1H-Pyrazolo[3,4-*b*] pyridine inhibitors of cyclin-dependent kinases, *Bioorg. Med. Chem. Lett.*, 2003, **13**, 1133–1136.
12 M. L. S. O. Lima, C. B. Braga, T. B. Becher, M. Odriozola-Gimeno, M. Torrent-Sucarrat, I. Rivilla, F. P. Cossío, A. J. Marsaioli and C. Ornelas, Fluorescent Imidazo[1,2-a] pyrimidine Compounds as Biocompatible Organic Photosensitizers that Generate Singlet Oxygen: A Potential

Tool for Phototheranostics, *Chem.–Eur. J.*, 2021, **27**, 6213–6222.

13 J. T. Sarmiento and J. Portilla, Current advances in chemosensors diazoles-based for CN– and F– detection, *Curr. Org. Synth.*, 2023, **20**, 61–79.

14 P. Moskwa, A. Kolbus, T. Uchacz, A. Danel and K. Gałczy, Fluorescent Sensor Based on 1H-Pyrazolo[3,4-*b*]quinoline Derivative for Detecting Zn2+ Cations, *Molecules*, 2024, **29**, 823.

15 J. Orrego-Hernández, C. Lizarazo, J. Cobo and J. Portilla, Pyrazolo-fused 4-azafluorenones as key reagents for the synthesis of fluorescent dicyanovinylidene-substituted derivatives, *RSC Adv.*, 2019, **9**, 27318–27323.

16 M. García, I. Romero and J. Portilla, Synthesis of Fluorescent 1,7-Dipyridyl-bis-pyrazolo[3,4-*b*:4′,3′-*e*]pyridines: Design of Reversible Chemosensors for Nanomolar Detection of Cu2+, *ACS Omega*, 2019, **4**, 6757–6768.

17 N. Medishetti, A. Kale, J. B. Nanubolu and K. Atmakur, Iron(III)chloride induced synthesis of pyrazolopyridines & quinolines, *Synth. Commun.*, 2020, **50**, 3642–3651.

18 X. Y. Miao, Y. J. Hu, F. R. Liu, Y. Y. Sun, D. Sun, A. X. Wu and Y. P. Zhu, Synthesis of Diversified Pyrazolo[3,4-*b*]pyridine Frameworks from 5-Aminopyrazoles and Alkynyl Aldehydes *via* Switchable C≡C Bond Activation Approaches, *Molecules*, 2022, **27**, 6381.

19 R. F. Barghash, W. M. Eldehna, M. Kovalová, V. Vojáčková, V. Kryštof and H. A. Abdel-Aziz, One-pot three-component synthesis of novel pyrazolo[3,4-*b*]pyridines as potent antileukemic agents, *Eur. J. Med. Chem.*, 2022, **227**, 113952.

20 E. Galarraga, N. Urdaneta, K. J. Gutierrez and J. C. Herrera, In vitro cytotoxicity of hydrazones, pyrazoles, pyrazolo-pyrimidines, and pyrazolo-pyridine synthesized from 6-substituted 3-formylchromones, *Z. Naturforsch., B: Chem. Sci.*, 2015, **70**, 305–310.

21 G. L. Beutner, J. T. Kuethe, M. M. Kim and N. Yasuda, Expedient synthesis of 3-alkoxymethyl- And 3-aminomethyl-pyrazolo[3,4-*b*]pyridines, *J. Org. Chem.*, 2009, **74**, 789–794.

22 T. Denzel and H. Höhn, Synthese von 1H-Pyrazolo[3,4-*b*] pyridin-5-ketonen, *Arch. Pharm.*, 1975, **1106**, 486–503.

23 M. Lácová, A. Puchala, E. Solčanyova, J. Lac, P. Koiš, J. Chovancová and D. Rasala, 3-formylchromones IV. The rearrangement of 3-formylchromone enamines as a simple, facile route to novel pyrazolo[3,4-*b*]pyridines and the synthetic utility of the latter, *Molecules*, 2005, **10**, 809–821.

24 S. V. Ryabukhin, A. S. Plaskon, D. M. Volochnyuk and A. A. Tolmachev, Chlorotrimethylsilane-mediated synthesis of functionalized fused pyridines: Reaction of 3-formylchromones with electron-rich aminoheterocycles, *Synthesis*, 2007, 1861–1871.

25 N. R. Misra, S. D. Kimball, D. B. Rawlins, K. R. Webster and I. Bursuker, Use of pyrazolo[3,4-*b*]pyridine as cyclin dependant kinase inhibitors, WO1999030710, 2007.

26 J. C. Castillo, A. Tigreros and J. Portilla, 3-Formylpyrazolo [1,5-a]pyrimidines as Key Intermediates for the Preparation of Functional Fluorophores, *J. Org. Chem.*, 2018, **83**, 10887–10897.

27 J. C. Castillo, H. A. Rosero and J. Portilla, Simple access toward 3-halo- and 3-nitro-pyrazolo[1,5-a]pyrimidines through a one-pot sequence, *RSC Adv.*, 2017, **7**, 28483–28488.

28 S. Aranzazu, A. Tigreros, A. Arias-G, J. Zapata-Rivera and J. Portilla, BF3-Mediated Acetylation of Pyrazolo[1,5-a] pyrimidines and Other π-Excedent (N-Hetero)arenes, *J. Org. Chem.*, 2022, **87**, 9839–9850.

29 CCDC 2358586 (**2a**), 2358587 (**2b**), 2358589 (**2b′**), and 2358588 (**3a**) contain the supplementary crystallographic data for this paper.

30 U. Krishnan, S. Manickam and S. K. Iyer, BF3 detection by pyrazolo-pyridine based fluorescent probe and applications in bioimaging and paper strip analysis, *J. Mol. Liq.*, 2023, **385**, 122413.

31 M. L. S. O. Lima, C. B. Braga, T. B. Becher, M. Odriozola-Gimeno, M. Torrent-Sucarrat, I. Rivilla, F. P. Cossío, A. J. Marsaioli and C. Ornelas, Fluorescent Imidazo[1,2-a] pyrimidine Compounds as Biocompatible Organic Photosensitizers that Generate Singlet Oxygen: A Potential Tool for Phototheranostics, *Chem.–Eur. J.*, 2021, **27**, 6213–6222.

32 S. Velázquez-Olvera, H. Salgado-Zamora, M. Velázquez-Ponce, E. Campos-Aldrete, A. Reyes-Arellano and C. Pérez-González, Fluorescent property of 3-hydroxymethyl imidazo [1,2-a]pyridine and pyrimidine derivatives, *Chem. Cent. J.*, 2012, **6**, 1–9.

33 V. V. Fedotov, M. I. Valieva, O. S. Taniya, S. V. Aminov, M. A. Kharitonov, A. S. Novikov, D. S. Kopchuk, P. A. Slepukhin, G. V. Zyryanov, E. N. Ulomsky, V. L. Rusinov and V. N. Charushin, 4-(Aryl)-Benzo[4,5] imidazo[1,2-a]pyrimidine-3-Carbonitrile-Based Fluorophores: Povarov Reaction-Based Synthesis, Photophysical Studies, and DFT Calculations, *Molecules*, 2022, **27**, 8029.

34 A. Tigreros, J. C. Castillo and J. Portilla, Cyanide chemosensors based on 3-dicyanovinylpyrazolo[1,5-a] pyrimidines: Effects of peripheral 4-anisyl group substitution on the photophysical properties, *Talanta*, 2020, **215**, 120905.

35 M. Homocianu, Exploring solvatochromism: A comprehensive analysis of research data, *Microchem. J.*, 2024, **198**, 110166.

36 A. Tigreros, M. Macías and J. Portilla, Structural, Photophysical, and Water Sensing Properties of Pyrazolo [1,5-a]pyrimidine-Triphenylamine Hybrid Systems, *ChemPhotoChem*, 2022, **6**, e202200133.

37 A. Tigreros, M. Macías and J. Portilla, Expeditious ethanol quantification present in hydrocarbons and distilled spirits: Extending photophysical usages of the pyrazolo[1,5-a]pyrimidines, *Dyes Pigm.*, 2022, **202**, 110299.

38 B. Valeur, *Molecular Fluorescence: Principles and Applications*, Wiley-VCH Verlag GmbH, Weinheim, Germany, 2001, vol. 1.

39 O. A. Kucherak, P. Didier, M. Yves and A. S. Klymchenko, Fluorene Analogues of Prodan with Superior Fluorescence Brightness and Solvatochromism, *J. Phys. Chem. Lett.*, 2010, **1**, 616–620.
40 E. Benedetti, L. S. Kocsis and K. M. Brummond, Synthesis and photophysical properties of a series of cyclopenta[*b*] naphthalene solvatochromic fluorophores, *J. Am. Chem. Soc.*, 2012, **134**, 12418–12421.
41 A. D. Becke, Density-functional thermochemistry. III. The role of exact exchange, *J. Chem. Phys.*, 1993, **98**, 5648–5652.
42 R. Dennington, T. A. Keith and J. M. Millam, *GaussView*, 2019.